NiTiSn a material of technological interest: Ab initio calculations of phase stability and defects

ARTICLE *in* INTERMETALLICS · MARCH 2014

Impact Factor: 2.13 · DOI: 10.1016/j.intermet.2013.10.016

3 AUTHORS:

Catherine Colinet
French National Centre for Scientific Resea…
137 PUBLICATIONS **1,732** CITATIONS
SEE PROFILE

Philippe Jund
Université de Montpellier
94 PUBLICATIONS **1,546** CITATIONS
SEE PROFILE

J.-C. Tédenac
Université de Montpellier
308 PUBLICATIONS **1,887** CITATIONS
SEE PROFILE

Intermetallics 46 (2014) 103–110

Contents lists available at ScienceDirect

Intermetallics

journal homepage: www.elsevier.com/locate/intermet

NiTiSn a material of technological interest: Ab initio calculations of phase stability and defects

Catherine Colinet [a], Philippe Jund [b], Jean-Claude Tédenac [b,*]

[a] Science et Ingénierie des Matériaux et Procédés, Grenoble INP, UJF, CNRS, 38402 Saint Martin d'Hères Cedex, France
[b] ICGM – Université Montpellier 2, Place Eugène Bataillon, 34095 Montpellier, France

ARTICLE INFO

Article history:
Received 16 May 2013
Received in revised form
10 October 2013
Accepted 17 October 2013
Available online 28 November 2013

Keywords:
A. Intermetallics, miscellaneous
B. Thermodynamic and thermochemical properties
D. Defects: point defects
E. Ab-initio calculations
G. Thermoelectric power generation

ABSTRACT

First principles calculations of the structural, thermodynamic, electronic and vibrational properties of $C1_b$-NiTiSn half-Heusler compounds have been performed. The enthalpy of formation of $C1_b$-NiTiSn has been obtained. The phonon density of states has allowed to derive a value of the Debye temperature of the compound. The enthalpies of formation of point defects have been calculated using large supercells. Four sublattices have been introduced to account for the $C1_b$ structure and for the possibility of inserting atoms in the 4d Wyckoff positions of the $F\bar{4}3m$ structure. The most stable defects are I^{Ni} and V^{Ni}. The corresponding densities of states have been computed.

1. Introduction

During the last years, a great number of researches have been done in the so-called Heusler and Half-Heusler compounds. These compounds are a class of ternary intermetallics associating three elements in the following stoichiometric proportions 1:1:1 (Half-Heusler) or 2:1:1 (Full-Heusler). They are represented by the general formula XYZ and X_2XZ, where X and Y are transition elements and Z is a s or p element. From a structural point of view, Heusler compounds generally crystallizes in the $L2_1$ structure (space group $Fm\bar{3}m$ with Cu_2MnAl as prototype) while the Half Heusler crystallizes in the $C1_b$ structure (space group $F\bar{4}3m$ with MgAgAs as prototype). New properties and potential fields of applications emerge constantly [1] in these materials (topological insulators and spintronics are recent examples). The properties of many Heusler compounds can easily be predicted by the valence electron concentration (VEC). Nevertheless their extremely flexible electronic structure offers a lot of possibilities for tailoring materials for interesting physical applications [1].

Concerning the thermoelectric properties, it was demonstrated that a VEC equal to 18 leads to potential good materials. Since good thermoelectric materials are typically heavily doped semiconductors (such as degenerated semiconductors), the classes of materials which are presently under investigation include mainly half-Heusler compounds. Half-Heusler compounds like MNiSn (M = Ti, Zr, Hf) are reported to be narrow bandgap n type semiconductors (Eg = 0.1–0.5 eV) and they exhibit a high Seebeck coefficient (~−200 μV/K) and low electrical resistivity (~1 × 10−4 Ωm). Unfortunately at this time a relatively high thermal conductivity is known to be around 10 W/mK at 300 K [1–6]. A drastic decrease of the thermal conductivity K associated to good electronic transport properties is mandatory if this material is to be used in thermoelectric applications [7–9]. However the different physical properties of these compounds are not well established and it is necessary to make a global study of these materials. Nevertheless it is well known that experimental evaluation of phase stability, thermodynamic and electric properties of materials is time consuming. So it is interesting to perform a first step in the study of this compound by numerical simulations.

The purpose of the present paper is to evaluate the thermodynamic properties, the phase stability, the electronic structure and the stability of the possible defects in order to have a global vision on the ternary compound in the ternary NiTiSn.

The paper is organized in four sections. In section 1, a synthetic discussion of the theoretical methods is presented. In section 2, we

* Corresponding author. Tel.: +33 467143342; fax: +33 467144290.
E-mail address: tedenac@um2.fr (J.-C. Tédenac).

0966-9795/$ – see front matter © 2013 Elsevier Ltd. All rights reserved.
http://dx.doi.org/10.1016/j.intermet.2013.10.016

present the results concerning the thermodynamic properties (enthalpy of formation and enthalpy of mixing), bandgap calculations for the ideal structure. In section 3, the enthalpies of formation of the possible defects are calculated using various sizes of supercells. The energetic effect corresponding to each step of the relaxation process is discussed. Finally, in section 4, we summarize the main conclusions of our work.

2. Method and calculation tools

The density functional (DFT) calculations were performed with the Vienna ab initio simulation package (VASP) [10], making use of the projector augmented waves (PAW) technique [11, 12]. Within the generalized gradient approximation (GGA) we have used the Perdew–Burke–Ernzerhof parameterization (PBE) for the exchange correlation functional [13]. The calculations took into account the following valence configurations: (Ni $4s^2 3d^8$, Sn $4d^{10} 5s^2 5p^2$; Ti $3s^2 3p^6 3d^3 4s^1$). A plane-wave cut-off energy of 500 eV for each element and compound has been taken. For the Brillouin-zone integration, the Methfessel-Paxton [14] technique with a modest smearing of the one-electron levels (0.2 eV) was used. In the case of the conventional fcc cell, a Monkhorst-Pack [15] $15 \times 15 \times 15$ grid was used. The structure was fully relaxed and remains face centered cubic. The Vinet et al. [16] equation of state was used to obtain the equilibrium volume (Ω_0), the total energy (E), the bulk modulus (B) and the pressure derivative of the bulk modulus ($\partial B/\partial P$).

In the case of the defect formation energy calculations, various supercells were built: a 24 atoms supercell which is a $2 \times 2 \times 2$ primitive cell, a 81 atoms which is a $3 \times 3 \times 3$ primitive cell, a 96 atoms supercell which is a $2 \times 2 \times 2$ fcc conventional cell. A sufficient number of k-points was chosen in each case. The plane-wave cutoff energy was reduced to 350 eV for the calculation of the total energy of the supercells containing defects with a moderate loss of accuracy.

3. Results and discussion on the ideal Half Heusler compound NiTiSn

In the present calculations, the lattice constants, the enthalpy of formation, the total and partial densities of states (DOS), the phonon spectrum and the density of states have been calculated.

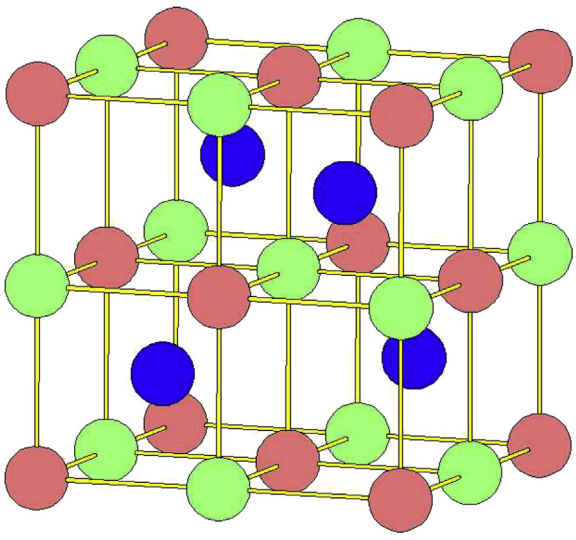

Fig. 1. Crystal structure of $C1_b$-NiTiSn showing the three occupied sub-lattices. Blue circles: Ni atoms, red circles Sn atoms, green circles Ti atoms.

Table 1
Structural data of *C1b*-NiTiSn compound compared to experimental data.

Lattice parameter (nm)	Bulk modulus	Debye temperature	Reference
0.5941			[18]
0.5937		417 K	[19]
0.5921			[20]
0.5930		335 K	[21]
0.59185			[22]
0.592890–0.592987			[23]
0.59332(6)			[24]
		283 K	[25]
0.5955	121 GPa	373 K	This work (PBE)

3.1. Crystal structure

The crystal structure of Half Heusler compounds is cubic, with the space group*F*4 3*m*, the Pearson symbol is *cF*12, the prototype is MgAgAs (structure $C1_b$). The structure is shown in Fig. 1 with the origin taken on a Sn atom [17].

First principles calculations were made by using the following crystallographic positions: Ni: 4*c* -43*m* (1/4 1/4 1/4); Ti : 4*b* 4 3*m* (1/2 1/2 1/2); Sn: 4*a* 4 3*m* (0 0 0). The calculated lattice constant can be compared to the experimental values in Table 1. One can observe that the calculated value of the lattice constant is close to the experimental data. Our value of the lattice parameter is also in agreement with recent theoretical calculations provided they are performed using the GGA approximation [22, 26–29, 31]. Calculations performed with the local density approximation (LDA) give smaller values of the lattice parameter [30–35].

In Fig. 2, we present the total energy per atom of the $C1_b$-NiTiSn compound as a function of the volume per atom. It shows the minimum volume (Vmin = 17.61 A^3/atom) and the minimum energy ($E_{min} = -6.38$ eV/atom). The fit of the curve with the Vinet equation of state [16] permits to obtain the bulk modulus B: we obtain a value close to 121.4 GPa. This value is in agreement with the values obtained in several theoretical calculations [27,35] provided that the GGA approximation is used. In the case of LDA approximation, the B value is higher [30,31,33].

In a cubic lattice, the number of independent elastic constants is three. In the case of $C1_b$-NiTiSn, we obtain: $c_{11} = 216.0$, $c_{12} = 75.9$, and $c_{44} = 62.3$ GPa. These values slightly differ from those obtained by Hichour et al. [30] probably due to the fact that these authors used the LDA approximation. They fulfil the mechanical stability conditions of a crystal possessing a cubic symmetry: $c_{11} > |.c_{12}|.$; $c_{11} + 2c_{12} > 0$; $c_{44} > 0$. Using this set of constants, the bulk modulus is obtained from $(c_{11} + 2c_{12})/3$ [31]. The obtained value of 122.6 GPa is in excellent agreement with

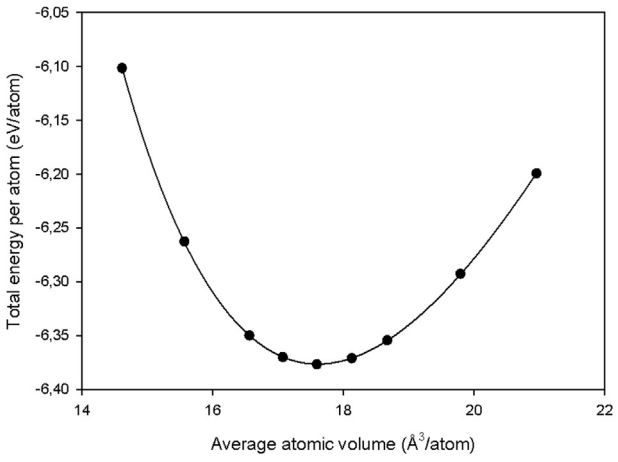

Fig. 2. Total energy vs. volume for the half Heusler $C1_b$-NiTiSn compound.

Table 2
Enthalpy of formation of NiTiSn compound in various structures. For the C1b-NiTiSn we took the notation of Ögüt and Rabe [32].

Compound	Space group	Pearson symbol	Struktur bericht designation	Prototype	Wyckoff positions	$\Delta_f H$ kJ/mol of atoms
α-NiTiSn	$F\bar{4}3m$	*cF*12	*C*1*b*	MgAgAs	Ni 4c, Sn 4a, Ti 4b	−53.0
β-NiTiSn	$F\bar{4}3m$	*cF*12	*C*1*b*	MgAgAs	Ni 4a, Sn 4c, Ti 4b	11.0
γ-NiTiSn	$F\bar{4}3m$	*cF*12	*C*1*b*	MgAgAs	Ni 4a, Sn 4b, Ti 4c	14.7
NiTiSn	$P6_3mc$	*hP*6	$B8_2$	LiGaGe	Ni 2b, Sn 2b, Ti 2a	−44.1
NiTiSn	$P\bar{6}2m$	*hP*9	*C*22	ZrNiAl	Ni 1b,Ni 2c,Sn 3f, Ti 3g	−34.7

the value of 121.4 GPa derived from the equation of state. The values of the shear moduli in the (100) and (110) planes are 62.3 and 70.0 GPa respectively. These results show that the cubic lattice is elastically anisotropic with an elastic anisotropy factor of 0.89. The values of the shear modulus, G, of the Young's modulus, E, and of the Poisson ratio, ν, are 65.3, 166.4, and 0.27 respectively.

The sets of elastic constants obtained for β-NiTiSn and γ-NiTiSn (see Table 2 for the Wyckoff positions of the atoms) show that these compounds are mechanically unstable. In the stable α-NiTiSn compound, the structure may be described by alternate (111) planes fully occupied by either Ti or Sn atoms. The Ni atoms are inserted between these planes and occupy one plane every two (see figures) and form regular tetrahedrons. The sequence is Ti/Ni/Sn/Ti/Ni/Sn. This situation is favoured by the fact that the atomic volume of Ni is smaller than the ones of Ti and Sn. In the case of β-NiTiSn for example, the large Sn atoms have to be inserted between Ti and Ni planes leading to a configuration that is not stable.

3.2. Enthalpy of formation of $C1_b$-NiTiSn

The energy of formation, $\Delta_f H(\mathrm{NiTiSn})$, per mol of atoms is obtained from the minimum total energy of the compound (expressed per mole of atoms) by subtracting the composition-weighted minimum total energies of pure fcc (A1) nickel, titanium in the hexagonal close packed (A3), and tin in the centred tetragonal (A5) structure:

$$\Delta_f H(\mathrm{NiTiSn}) = E^{\min}_{\mathrm{NiTiSn}} - \frac{1}{3}E^{\min}_{\mathrm{A1-Ni}} - \frac{1}{3}E^{\min}_{\mathrm{A3-Ti}} - \frac{1}{3}E^{\min}_{\mathrm{A5-Sn}} \quad (1)$$

At $T = 0$ K and $p = 10^5$ Pa, the enthalpy of formation equals the calculated formation energy when the (much smaller) zero-vibration contribution is ignored.

In Table 2, we also present the values of the enthalpy of formation of the NiTiSn compound in the MgAgAs-type structure by modifying the positions of Ni, Sn, and Ti on the three Wyckoff positions 4a, 4b and 4c of the $F\bar{4}3m$ space group (referred to β and γ by Ögüt and Rabe [33] and Onoue et al. [34]). Positive values of the enthalpies of formation are obtained when Ni atoms occupy the 4a positions whereas the Ti or Sn atoms occupy the 4b and 4c positions. The energy differences of the β and γ configurations with respect to the stable configuration denoted α have been calculated by Larson et al. [26]. Our values are in excellent agreement. In the stable configuration, the Ni atoms are surrounded by 4 Ti atoms and 4 Sn atoms at a distance of 2.58 Å.

We also calculated the enthalpy of formation of NiTiSn in two structural types, LiGaGe (*hP*6, space group $P6_3mc$) and ZrNiAl (*hP*9, space group $P\bar{6}2m$) in which equiatomic ternary compounds often crystallize [17]. By calculating the enthalpy of formation and testing the different positions of the atoms on the sites of these structures, we obtained the results indicated in column 6 of Table 2. It remains that the stable structure is really the MgAgAs prototype with Ni occupying the 4c, Sn the 4a and Ti the 4b Wyckoff positions.

The enthalpy of formation of the $C1_b$-NiTiSn compound is equal to −53.0 kJ/mol (see Table 2). This very negative value of the enthalpy of formation explains the stability of this compound with respect to the other ternary compounds existing in the ternary Ni–Ti–Sn system (by comparison of the stability of other possible ternary phases).

3.3. Electronic structure

We present in Fig. 3 the total electronic density of states of the perfect compound. In order to compare the behaviour of the perfect compound and the compound with intrinsic defects, we present also in Fig. 3 the partial DOS of Ni, Ti and Sn. As shown, $C1_b$-NiTiSn is a narrow band gap semiconductor, which is a priori favourable for thermoelectricity. The value of the gap is equal to 0.416 eV, while the experimental value of Aliev et al. [25] lies in the range 0.12 eV. A value between 0.4 and 0.45 eV for the gap is obtained in all the theoretical calculations which have been performed recently using the GGA functional [22, 24, 27, 28, 31]. A value between 0.47 and 0.51 eV is obtained in the LDA calculations [33, 30, 34, 32]. This unusual overestimation of the gap using GGA simulations with respect to the experimental gap is probably due to the fact that a perfect compound is considered in the calculations while the real compound used in the experiments contains defects and imperfections. Nevertheless, this needs still to be confirmed.

The bonding states below the Fermi level are predominantly of Ni-3d character while the antibonding states above the Fermi level are Ti-3d character. The partial densities of states where the s, p, d contributions have been displayed allow to conclude that the

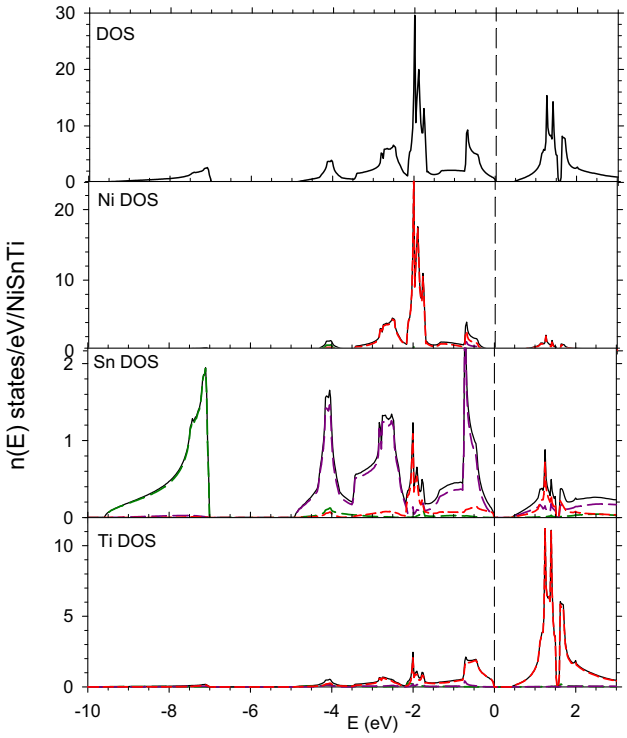

Fig. 3. From top to bottom: $C1_b$-NiTiSn total electronic density of states, Ni partial density of states, Sn partial density of states, Ti partial density of states. In the partial densities of states the s, p, and d contributions are represented by green, pink, and red dotted lines respectively.

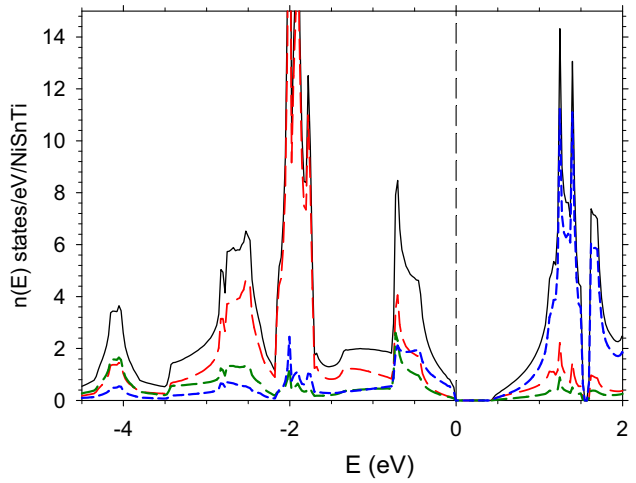

Fig. 4. Enlargement of the DOS and PDOS of C1$_b$-NiTiSn around the Fermi level.

PDOS of Ni and Ti are dominated by the d electrons while the PDOS of Sn consists of s and p contributions. From −9 to −7 eV the DOS is dominated by the Sn-5s states. These 5s states are separated from the Sn-5p states by an energy gap. The two first peaks below the Fermi level at −4 eV and −2.5 eV correspond to the hybridization between the Sn-p states and Ni-d states. The two other peaks at −2 and −0.75 eV are due to the hybridization between the Ni-d states, Ti-d states, and Sn p states. In Fig. 4, one can see that the contributions of Sn and Ti orbitals are clearly close to the valence band edge. This small but finite DOS at the Fermi level was already pointed out by Ögüt et al. [33], and is in agreement with the specific heat measurements [19,25]. These results agree also very well with previously published papers, particularly those of Tobola et al. [36], Hichour et al. [30], Onoue et al. [34], Ouardi et al. [22], Ameri et al. [32], and Wang et [27].

The electronic band structure is presented in Fig. 5. The overall band profile is in good agreement with previous calculations [27,30–33]. The calculated indirect band gap values are listed in Table 3. They are slightly lower than those obtained by Hichour et al. [30] who used the LDA approximation for the exchange-correlation potential.

The Bader charges of the atoms have been computed using the Bader analysis [36] in order to understand the charge transfer between the atoms in the structure. The calculation was made by using a cubic cell of 12 atoms. The results, reported in Table 4, show that there is a charge transfer from Ti to Ni atoms leading to an

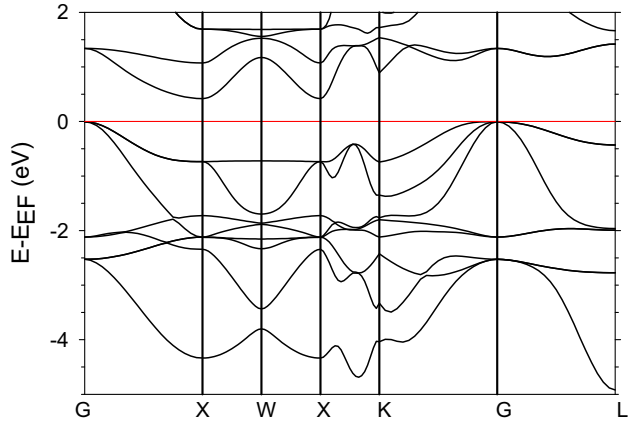

Fig. 5. Band structure of C1$_b$-NiTiSn along high-symmetry lines of the fcc Brillouin zone. The origin is taken at the top of the valence band.

Table 3
Calculated indirect band gaps (in eV) for NiTiSn in the C1b structure.

C1*b*-NiTiSn	Γ-X	Γ-W	Γ-K	Γ-L
Present work	0.416	1.170	0.888	1.414
Hichour et al.	0.468	1.27	0.965	1.487

Table 4
Bader charges calculated for *C1b*-NiTiSn.

Number of electrons in the isolated atom: N_i	Number of electrons in the compound: N_c	$N_c - N_i$
Ni (10 electrons-)	11.08	+1.08
Sn (14 electrons)	14.22	+0.22
Ti (12 electrons)	10.7	−1.3

almost Ni filled band. A smaller transfer from Ti atoms to Sn atoms is also observed. This is in agreement with charge-density calculations performed by Offernes et al. [37].

3.4. Phonon spectrum and Debye temperature

The phonon density of states and the phonon band structure were calculated using the Phonopy software [38]. They are presented in Figs. 6 and 7. The calculation of the Debye temperature was made according to the Debye approximation as shown in Fig. 6 and we found a value equal to 370 K. Experimental values of the Debye temperature have been derived by Aliev et al. [25], Kuentzler

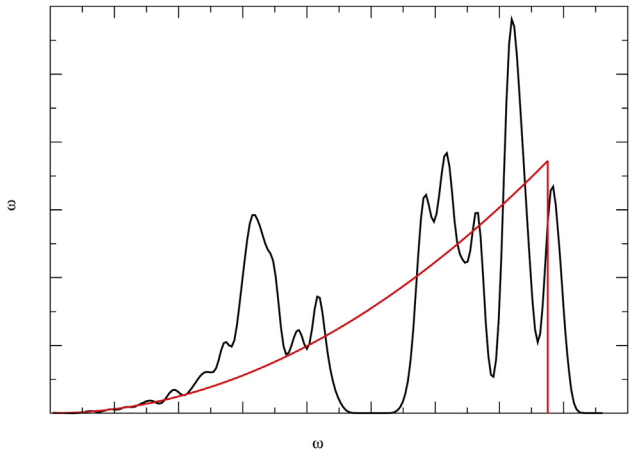

Fig. 6. Phonon density of states of C1$_b$-NiTiSn compound; Y-axis: g(ω) and X-axis: ω (THz).

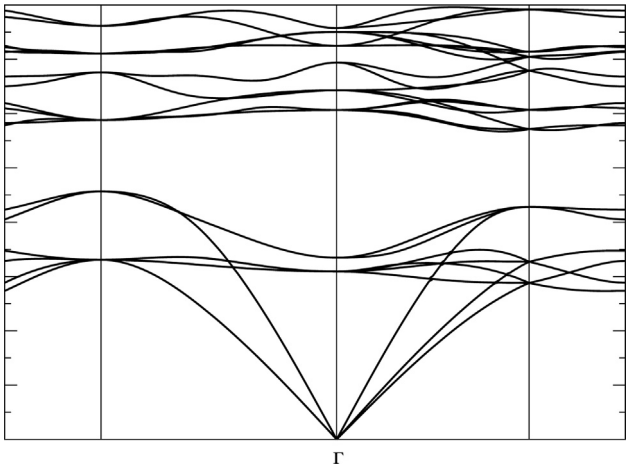

Fig. 7. Phonon band structure in the conventional fcc cell.

et al. [19], and Dhong [21] from Cp measurements at low temperature. These authors obtained respectively 283, 417, and 335 K for the Debye temperature. Our calculated value falls between the values reported by Kuentzler et al. [19] and Dhong [21], and is in good agreement with the calculated value of Hichour et al. [30] who derived the Debye temperature from the calculated values of the elastic constants.

The Helmholtz free energy of the compound $C1_b$-NiTiSn,$F_{vib}(V,T)$, is determined as a sum of the free energies of all phonons assuming that vibrations are independent [38]. If the phonon density of states g(ω) is known, the quasi-harmonic free energy per primitive unit cell [39] may be written as:

$$F_{vib}(V,T) = \int_0^\infty \left[\frac{\hbar\omega}{2} + k_B T \ln\left(1 - \exp\left(-\frac{\hbar(\omega)}{k_B T}\right)\right)\right] g(\omega) d\omega \quad (2)$$

The vibrational thermodynamic data have been calculated and are reported in Fig. 8.

4. Defects in half Heusler NiTiSn compound

The defect enthalpies of formation have been calculated in order to understand the doping effects in this material. Indeed, in the paper [40], the authors claim that the thermoelectric properties are strongly influenced by the defects in the structure, since they lead to a lowering of the thermal conductivity. According to the chemical properties of the elements, in the $C1_b$ structure, the most probable stable defects should be vacancies on each constituent site (they correspond typically to the thermal defects) and interstitial nickel which can partially occupy the 4d position of the $F4\,3m$ space group (positions occupied by Ni atoms in the $L2_1$ Heusler structure). We have performed defect formation energy calculations using variable sized supercells. In addition, in each case, the cell has been fully relaxed and we insured that it remains cubic. Therefore successive volume and atomic position relaxations have been performed. All the possible defects have been studied: vacancies, antisites and insertion of Ni, Sn, or Ti in 4d position of the $F4\,3m$ space group.

4.1. Enthalpy of formation of defects

The enthalpy of formation of the compound with defects is written as [41]:

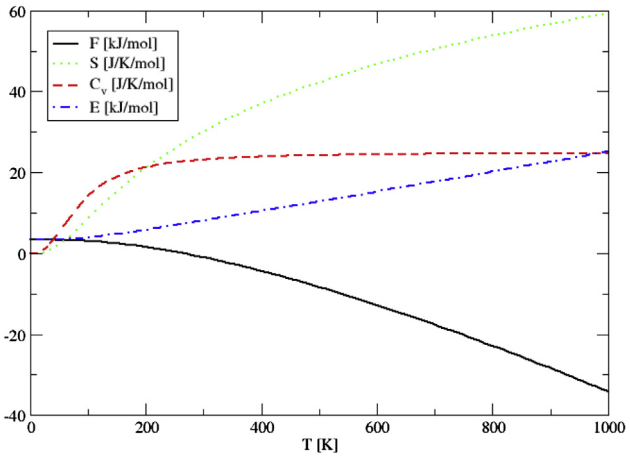

Fig. 8. Vibrational thermodynamic data of $C1_b$-NiTiSn. Frequency (THz) as a function of temperature (K).

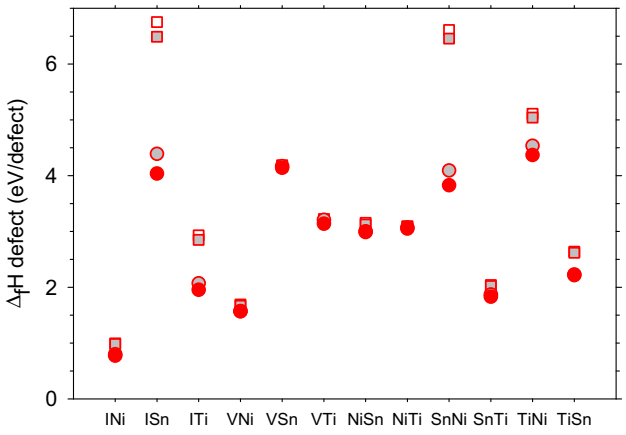

Fig. 9. Point defect enthalpies of formation at each step of the relaxation process in the case of a supercell of 81 atoms. Empty squares : without relaxation, grey filled squares : volume relaxation, grey filled circles : relaxation of the nearest neighbours of the defect (NN), red filled circles : relaxation of all the atoms in the cell.

$$\Delta_f H = \Delta_f H^\circ\left(Ni_{1/3}Sn_{1/3}Ti_{1/3}\right) + \sum_d X_d H_d \quad (3)$$

x_d is the atomic defect concentration, H_d is the defect formation enthalpy and $\Delta_f H^\circ(Ni_{1/3}Sn_{1/3}Ti_{1/3})$ is the enthalpy of formation of the perfectly ordered stoichiometric compound defined by relation (1). Let us point out that the point-defect volumes of formation have also been calculated and we have concluded that the influence of pressure on the defect enthalpies of reaction can be neglected at ordinary pressure.

The enthalpies of formation of the possible defects in the $C1_b$ structure (81-atom supercell) are presented in Fig. 9 at each step of the relaxation process. The energetic effect due to the volume relaxation is very small. In the second relaxation step, only the nearest neighbours (NN) of the defect have been allowed to relax. This energetic effect is very important. In the last step, all the atoms of the supercell have been allowed to relax. One can remark that the change of the defect enthalpy of formation is small. Therefore, we can conclude that the most important effect is due to the relaxation of the nearest neighbours of the defect.

In Fig. 10, the values of the defect enthalpies of formation obtained after full relaxation in different supercells containing 24, 81

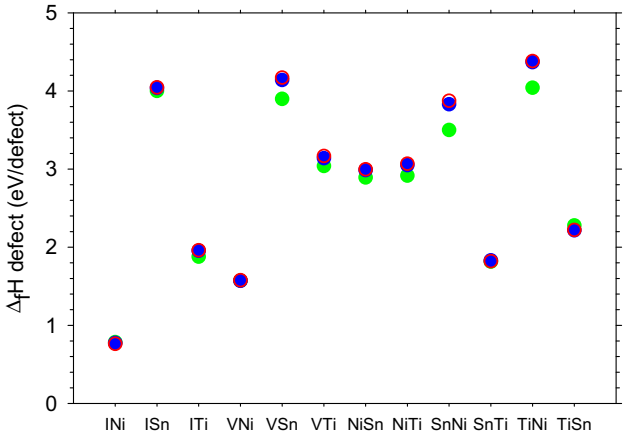

Fig. 10. Point defect enthalpies of formation after full relaxation of the supercell. Green circles: 24 atom supercell, blue circles: 81 atom supercell, empty red circles: 96 atom supercell.

Table 5
Enthalpies of formation of the defects after full relaxation expressed in eV/defect.

Defect	I^{Ni}	V^{Ni}	Sn^{Ti}	I^{Ti}	Ti^{Sn}	Ni^{Sn}	Ni^{Ti}	V^{Ti}	Sn^{Ni}	I^{Sn}	V^{Sn}	Ti^{Ni}
Cell.81	0.77	1.57	1.83	1.95	2.22	2.99	3.05	3.14	3.83	4.04	4.14	4.37
Cell.96	0.76	1.58	1.82	1.96	2.22	3.00	3.07	3.17	3.87	4.05	4.17	4.38

and 96 atoms are compared. We find that the results are identical for the 81 and 96 atom supercells and even with a calculation in the supercell containing 24 atoms the results show the same tendency as in the larger cells.

Numerical values are summarized in Table 5. It appears that the most stable defect is the Ni interstitial, this situation is due to the existence of the fourth sub-lattice (4d sites of the structure which are empty in the $C1_b$ structure (half-Heusler) and fully occupied in the $L2_1$ structure (Heusler)). Since the occupancy of this position leads to a change in the space group, one cannot observe a continuous series of solid solutions as it is shown in [38] but only randomly distributed defect positions. Finally the calculations lead to the following sequence in the relative stability of the defects:$I^{Ni} < V^{Ni} < Sn^{Ti} < Ti^{Sn} < I^{Ti}$ (other defects are not realistic). The enthalpies of formation of the supercells of 81 atoms containing one defect after full relaxation are shown in a spatial ternary diagram (Fig. 11). The difference of stabilities is very large between I_{Ni} and the other defects.

Recently Hazama et al. [42] performed ab-initio calculations of the formation energy of defects in $C1_b$-NiTiSn considering the five following cases: V^{Sn}, V^{Ti}, Ni^{Ti}, Ni^{Sn}, and I^{Ni}. The order of magnitude of the formation energies of defects they have obtained compare well with ours. In addition, they computed the DOS in each case and compared with the one obtained with X ray photoemission spectroscopy measurements. The comparison allows Hazama et al. [42] to conclude that excess Ni atoms stay in the vacant 4d sites of the structure.

4.2. Electronic structure with the most stable defects

Recently Zhu et al. [29] studied the effect of vacancies in $C1_b$-NiTiSn and obtained local magnetic moments induced into the nonmagnetic host materials for all types of isolated vacancies except for the Ni vacancy. We performed spin-polarized calculations in these cases using a supercell containing 96 atoms. The electronic densities displayed in Fig. 12 are very similar to those obtained by Zhu et al. [29]. We also obtained the same magnetic moment in the supercell without and with relaxation. However we cannot reproduce the same behaviour when using a supercell containing 81 atoms. We also performed spin-polarized calculations in the case of one Ni atom inserted in the 4d position. The electronic density of states is displayed in Fig. 13. A Ni atom inserted in the 4d Wyckoff position has hardly any effect on the magnetic state of the $C1_b$-NiTiSn host.

We have also calculated the DOS and the partial DOS for the most stable defects: V^{Ni} and I^{Ni}. The most interesting result concerns the nickel interstitial defect which is located on the 4d sites. The partial DOS of the atoms which are nearest neighbour (NN) or not of the defect are displayed in Fig. 14. This defect leads to a localized level inside the gap close to the Fermi level and to a n-type doping behaviour with a high carrier concentration. In the case of the Ni vacancy, no special feature appears.

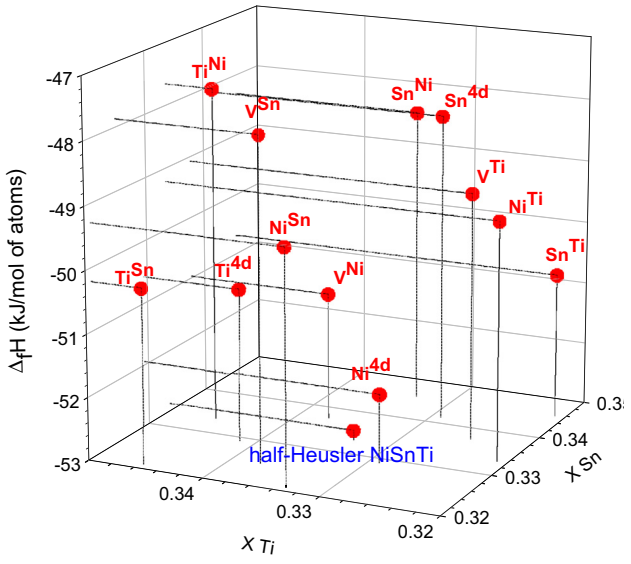

Fig. 11. Spatial diagram of the enthalpy of formation of a 81 atom supercell containing one defect.

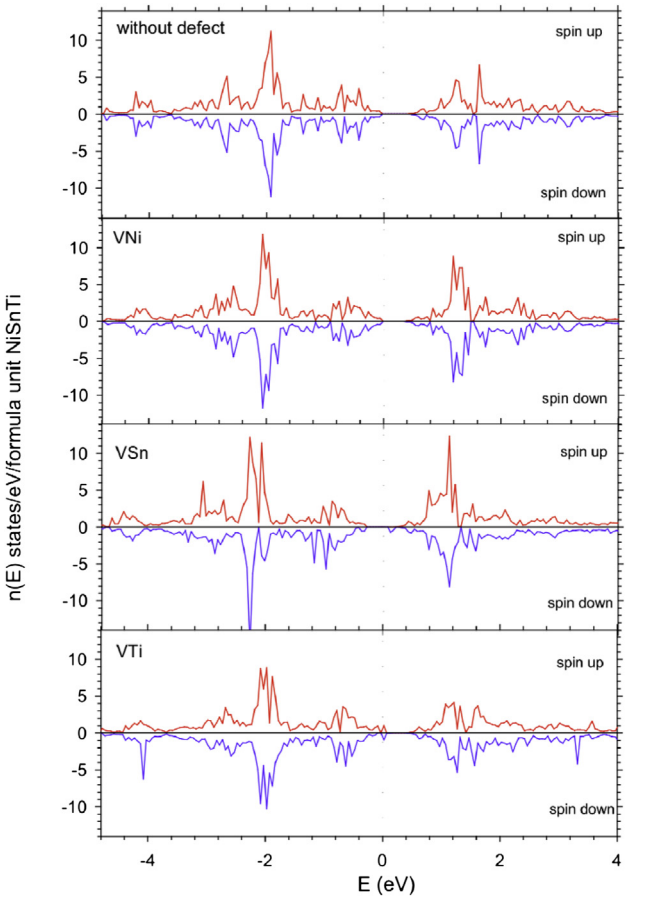

Fig. 12. Spin polarized electronic total density of states of the 96 atom supercell. From top to bottom : without defect, with one Ni vacancy, with one Sn vacancy, and with one Ti vacancy.

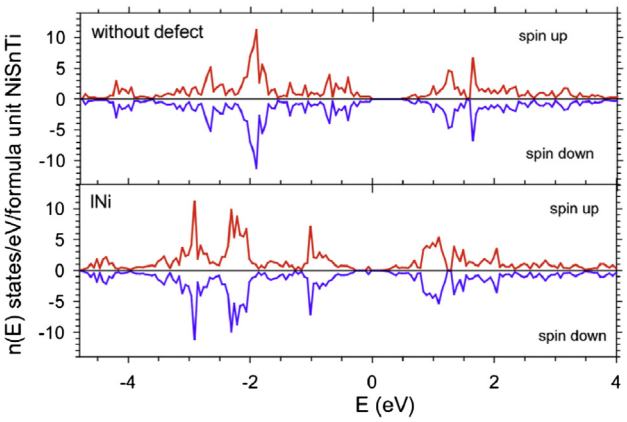

Fig. 13. Spin polarized total electronic density of states of the 96 atom supercell. From top to bottom: without defect, with interstitial Ni on 4d sites of *F*4 3*m*.

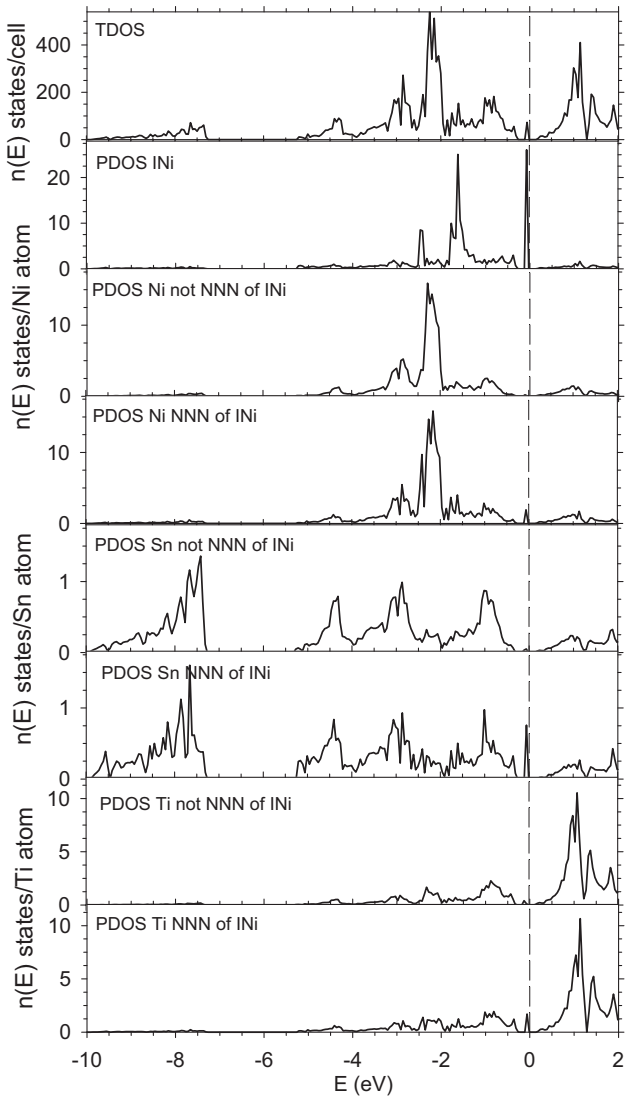

Fig. 14. Electronic density of states when considering nickel in the 4d interstitial position. From the top to the bottom: total density of states, partial density of states of Ni in interstitial position, partial density of states of Ni not NN of the Ni in interstitial position, partial density of states of Ni NN of the Ni in interstitial position, partial density of states of Sn not NN of the Ni in interstitial position, partial density of states of Sn NN of the Ni in interstitial position, partial density of states of Ti not NN of the Ni in interstitial position, partial density of states of Ti NN of the Ni in interstitial position.

Inspection of Fig. 14 allows to draw some conclusions. When the vacancy is exclusively on the titanium sites, we observe that the Fermi level is located inside the valence band showing a p type doping. Concerning the nickel vacancies, these defects lead also to a p type semi-conductor. When the vacancy is on the tin sites, one can see that the Fermi level shifts toward the conduction band showing a n type conduction. According to previous published results [43], it should lead to a decrease of the thermal conductivity.

5. Conclusions

We have performed detailed investigations of the structural, thermodynamic, electronic and vibrational properties of the half-Heusler NiTiSn compound using first principles calculations in the GGA approximation. The most relevant conclusions are as follows:

- The enthalpy of formation of $C1_b$-NiTiSn is −53.0 kJ/mol.atoms with the reference states FM-A1-Ni, A3-Ti, and A5-Sn.
- The computed phonon density of states of $C1_b$-NiTiSn permits an estimation of the Debye temperature of 370 K. The vibrational thermodynamic properties of the compound have been calculated as a function of temperature.
- We performed ab-initio calculations of enthalpies of formation of point defects by investigating all possible defects: vacancies, antisites, and insertion of atoms in the 4d sites of the *F*4 3*m* structure. Large supercells have been built for this purpose. The energetic effects associated to relaxations (volume and positions of the atoms) have been studied. The most stable defects are Ni vacancies and Ni atoms in interstitial position. The corresponding electronic densities of state have been computed. The insertion of Ni atom leads to a localized level inside the gap close to the Fermi level and to a n-type doping behaviour.

Acknowledgements

The computer resources used in this work have been sponsored by “La Fondation EADS”. We thank also the computer centers CINES and hpc@lr in Montpellier for their support.

References

[1] Graf Tanja, Felser Claudia, Parkin Stuart SP. Prog Solid State Chem 2011;39:1–50.
[2] Uher C, Yang J, Hu S, Morelli DT, Meisner GP. Phys Rev B 1999;59:8615–21.
[3] Kimura Y, Ueno H, Mishima Y. J Electron Mater 2009;38:934.
[4] Xie W, Jin Q, Tang X. J Appl Phys 2008;103:043711.
[5] Schwall M, Balke B. Appl Phys Lett 2011;98:042106.
[6] Mastronardi K, Young D, Wang C-C, Khalifah P, Cava RJ, Ramirez AP. Appl Phys Lett 1999;74:1415.
[7] Xia Y, Ponnambalam V, Bhattacharya S, Pope AL, Poon SJ, Tritt TM. J Phys Condens Matter 2001;13:77–89.
[8] Bhattacharya S, Pope AL, Littleton RT, Tritt TM, Ponnambalam V, Xia Y, et al. Appl Phys Lett 2000;77:2476.
[9] Qui P, Huang X, Chen X, Chen L. J Appl Phys 2009;106:103703.
[10] Kresse G, Furthmüller J. Comp Mater Sci 1996;6:15;
Phys Rev B 54 (1996) 11169.
[11] . Blöchl PE. Phys Rev B 1994;50:17953.
[12] Kresse G, Joubert D. Phys Rev B 1998;59:1758.
[13] Perdew JP, Burke S, Ernzerhof M. Phys Rev Lett 1996;77:3865.
[14] Methfessel M, Paxton AT. Phys Rev B 1989;40:3616.
[15] Monkhorst HJ, Pack JD. Phys Rev B 1976;135:5188.
[16] Vinet P, Rose JH, Ferrante J, Smith JR. J Phys Condens Matter 1989;1:1941.
[17] Villars P, Calvert LD. Pearsons handbook of crystallographic data for intermetallic phases. Metals Park, OH: ASM; 2010/2011. Release.
[18] Jeitschko W. Metall Trans 1970;1:3159–62.
[19] Kuentzler R, Clad R, Schmerber G, Dossmann Y. J Magn Magn Mater 1992;104–107:1976–8.
[20] Pierre J, Skolozdra RV, Gorelenko YK, Kouacou M. J Magn Magn Mater 1994;134:95–105.
[21] Dhong B. Physical metallurgy and properties of TiNiSn and PtMnSb. Iowa State University; 1997. Ph.D. Thesis.

[22] Ouardi S, Fecher GH, Balke B, Kozina X, Styganyuk G, Felser C, et al. Phys Rev B 2010;82:085108.
[23] Birkel CS, Zeier WG, Douglas JE, Lettiere BR, Mills CE, Seward G, et al. Chem Mater 2012;24:2558–65.
[24] Romaka VA, Rogl P, Romaka VV, Hlil EK, Stadnyk Yu V, Budgerak SM. Semiconductors 2011;45:850–6.
[25] Aliev FG, Kozyrkov VV, Moshchalkov VV, Scolozdra RV, Durczewski K. Z Phys B- Condensed Matter 1990;80:353–7.
[26] Larson P, Mahanti SD, Kanatzidis MG. Phys Rev B 2000;62:12754–62.
[27] Wang LL, Miao L, Wang ZY, Wei W, Xiong R, Liu HJ, et al. J Appl Phys 2009;105:013709.
[28] Hazama H, Asahi R, Matsubara M, Takeuchi T. J Electron Mater 2010;39:1549–53.
[29] Zhu Z, Cheng Y, Schwingenschlögl U. Phys Rev B 2011;84:113201.
[30] Hichour M, Rached D, Khenata R, Rabah M, Merabet M, Reshak AH, et al. Chem Solids 2012;73:975–81.
[31] Zhu R, Pan E, Chung PW, Cai X, Liew KM, Buldum A. Semicond Sci Technol 2006;21:907.
[32] Ameri M, Touia A, Khenata R, Al-Douri Y, Baltache H. Optik 2013;124:570–4.
[33] . Ögüt S, Rabe KM. Phys Rev B 1995;51:10443–53.
[34] Onoue M, Ishii F, Oguchi T. J Phys Soc Jpn 2008;77:054706.
[35] Tobola J, Pierre J, Kaprzyk S, Skolozdra RV, Kouacou MA, Mag J. Mag Mater 1996;159:192–200.
[36] Bader RFW. Atoms in molecules – a quantum theory. New York: Oxford University Press; 1990.
[37] Offernes L, Ravindran P, Kjekshus A. J Alloys Compd 2007;439:37–54.
[38] Togo A, Oba F, Tanaka I. Phys Rev B 2008;78:134106.
[39] Grimvall G. Thermophysical properties of materials. Elsevier; 1999. pp. 79–111.
[40] Viennois R, Jund P, Colinet C, .Tedenac J-C. J Sol State Chem 2012;193:133–6.
[41] Korzhavyi PA, Ruban AV, Lozovoi AY, Vekilov YK, Abrikosov IA, Johansson B. Phys Rev B 2000;61:6003.
[42] Hazama H, Matsubara M, Asahi R, Takeuchi T. J Appl Phys 2011;110:063710.
[43] Bhandari CM. In: Rowe DM, editor. CRC handbook of thermoelectrics 1995. pp. 55–65. CRC, Boca Raton.